NH_3 and SF_6 detection based on long-wave infrared pyroelectric detector

Huanhuan Wang[a], Linfang Xu[a*], Weiguo Chen[a], Kristel Pei Xuan Wee[a], Anmin Kong[a], Md Hazwani Khairy Md Husni[a], Zhonghua Gu[a], Chong Pei Ho[a], Qingxin Zhang[a], Doris Keh Ting Ng[a#]
[a]Institute of Microelectronics (IME), Agency for Science, Technology and Research (A*STAR), 2 Fusionopolis Way, Innovis #08-02, Singapore 138634, Republic of Singapore

ABSTRACT

Thermal infrared emitter and pyroelectric detector are two common main components to provide effective gas detection in non-dispersive infrared (NDIR) sensor. Commercially available emitters often have low emission power above 5 μm, limiting gas sensing in the long-wave infrared (LWIR), including ammonia (NH_3) and sulfur hexafluoride (SF_6). In this work, we make use of an in-house scandium aluminum nitride (ScAlN) pyroelectric detector with high absorption of ~85% in the wavelength range from 10.5 to 11 μm to compensate for the low emitter power at the system level. The pyroelectric detector based NDIR sensor demonstrates reliable gas responses for both NH_3 and SF_6, with the detection limit of 44 and 6 ppm respectively. The relatively higher detection limit of NH_3 is due to its weak infrared absorption. To further investigate this, we demonstrate sensors using 10 cm and 20 cm long gas channel paths. When the gas path length is 20 cm, the system achieves a detection limit of 19 ppm, significantly improved compared to 44 ppm with 10 cm gas path length. The effective absorption coefficient of NH_3 is calculated to be ~0.025 based on the modified Beer-Lambert law, indicating strong sensing capability. This pyroelectric detector-based gas sensor shows great potential for real-time SF_6 leak detection in industrial processes, as well as NH_3 monitoring in clean energy.

Keywords: ScAlN pyroelectric detector, NDIR sensor, long wave infrared sensing, gas path length

1. INTRODUCTION

NH_3 and SF_6 monitoring are critical for environmental safety as they can either cause serious health problems [1] or pose significant greenhouse warming potential.[2] NH_3 monitoring is not only crucial for environmental protection, but also important for H_2 energy storage and transportation, both in Singapore and globally. It is being increasingly explored in clean energy as a hydrogen carrier due to its higher energy density compared to hydrogen. Therefore, NH_3 sensing technologies are important for helping reduce emissions and support the shift to cleaner energy.

One such technology is the NDIR sensor, which has emerged as an effective tool for accurate NH_3 detection.[3, 4] In NDIR, we take advantages of molecular optical absorption effect, where NH_3 and SF_6 concentration can be measured based on the absorbed light. When light is emitted from the source, it propagates along the gas channel. As NH_3 and SF_6 have unique absorption fingerprints, the molecules vibrate and absorb the specific wavelength infrared light. Such molecule-light interaction modifies the light intensities and is measurable at the detector end. Therefore, the final output light intensity provides the gas concentration information, which is decided by the Beer-Lambert law [5]:

$$T = I/I_0 = exp(-\varepsilon\ c\ l), \quad (1)$$

where I_0 is the initial input light intensity, I represents the output intensity of light after passing through the gas channel, where the light interacts with the target gas. ε is the molar absorptivity, c is the gas concentration, and l is the interaction length. For a given gas and a fixed optical path l, with known gas concentrations, the detector responses can be used to determine unknown concentrations after data training.[6]

However, reports on NH_3 gas testing have not been as extensive as other more common greenhouse gases such as carbon dioxide (CO_2). This is partly due to the challenges of handling NH_3 safely in the lab, requiring stringent protective measures to maintain very low concentrations, ensuring no exposure to humans or the environment. Additionally, due to the low absorbance of ammonia in the 3.0 to 3.5 μm wavelength range,[7] detecting NH_3 using conventional NDIR sensors is challenging. Although NH_3 molecules have a strong absorption line at a wavelength of 10.7 μm, the low-power emission of currently commercially available emitters above 10 μm remains another obstacle.

*xu_linfang@a-star.edu.sg; [#]doris_ng@a-star.edu.sg; https://www.a-star.edu.sg/ime;

In this work, we report a pyroelectric detector with high absorption above 10 µm to compensate the low emitter power at the system level. The detector operates based on a 20% ScAlN pyroelectric thin film sandwiched between top and bottom electrodes.[6] At around 10.5 to 11 µm, the absorption is ~85%, which is ideal for NH_3 detection, with characteristic absorption wavelength 10.7 µm which is our wavelength of interest. Based on this, we further developed a laboratory-safe NH_3 detection method, including a bubbling system, a gas sensor system, and a suitable exhaust. With a 20 cm gas channel configuration, the calculated effective absorption coefficient is as high as 0.02. As a result, the detection limit reaches 19 ppm.

2. NDIR SENSOR AND PYROELECTRIC DETECTOR

2.1 NDIR gas sensor

Figure 1 shows the schematic of the gas testing setup. NH_3 (or SF_6) as target gas of interest and N_2 is used as reference gas to mix after passing through respective mass flow controllers (MFC) to achieve desired gas concentrations. The gas then flows through an NDIR gas sensor, which typically consists of a light source, a gas channel, and a detection system. The EMIR MEMS based infrared source from Axetris is used as light source in this work. The gas channel is designed to 10 cm or 20 cm long with 1 cm inner diameter to perform gas testing. An optical filter is added before the detector to sense gas response at characteristic wavelength. The detector end is an in-house Sc-AlN pyroelectric detector that generates a small current in response to instantaneous temperature changes. The electrical circuitry is designed to convert the detector's output current to voltage via a low-noise transimpedance amplifier, after which the signal is further amplified and filtered before being sent to an 18-bit analog-to-digital converter (ADC). The digitized data is then processed by a microcontroller (MCU). The entire sensor system is powered by a laptop through a 5 V supply via a universal serial bus (USB) cable, which is also used for data transfer between the sensor and the computer.

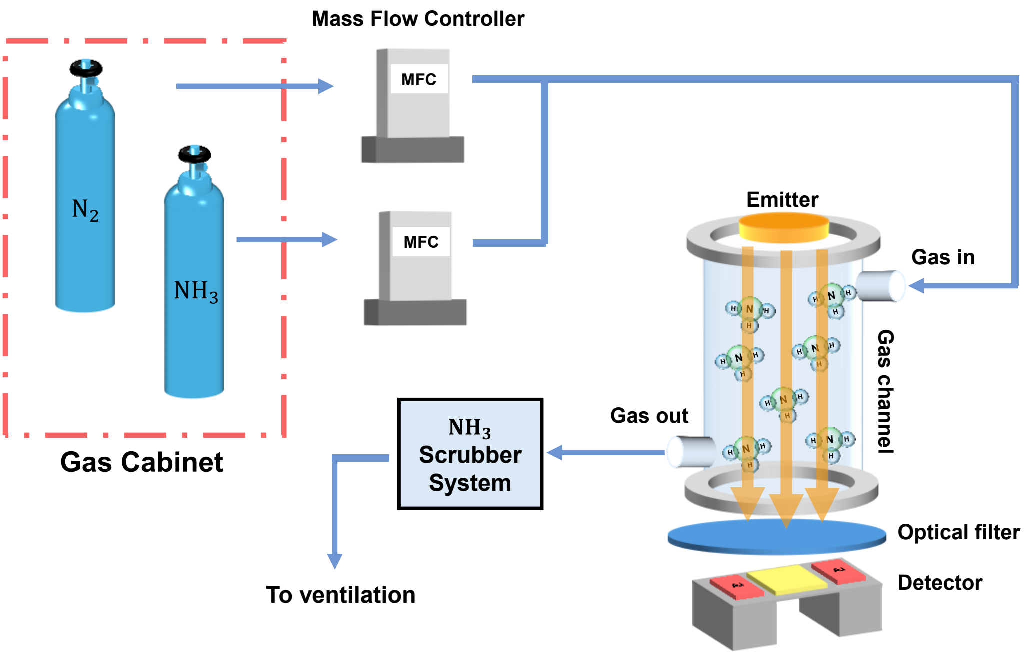

Figure 1. Schematic diagram of the NDIR gas testing system and the membrane pyroelectric detector.

2.2 ScAlN-based pyroelectric detector

Figure 2a shows the microscopy image of the top of 20% ScAlN-based pyroelectric detector. The center part is the stack of active area ~560 µm x 560 µm. The outer part is the ribs to improve the mechanical strength of the membrane structure.[8] The top (titanium nitride, TiN) and bottom (molybdenum, Mo) electrode lines are seen in Figure 2a as well. The metal electrode lines are connected to metal contact for the electrical signal extraction. Figure 2b shows the bottom view of the membrane detector, where the membrane size is clearly measured and reflected in the image. The device is with good structure integrity on both sides.

Figure 2c presents the Fourier transform infrared (FTIR) spectra for the detector. Absorption is derived from the FTIR transmission and reflection spectra.[9] The inset highlights the interactions of light with the detector stack: it can either pass through, reflect, or be absorbed. For optimal performance, we aim for maximum absorption of the detector layer for high detection sensitivity. Here a high absorption of ~85% at ~10.5 to 11 μm wavelengths is achieved, which includes our wavelength region of interest where NH_3 (10.7 μm) and SF_6 (10.6 μm) characteristic absorption lines occur. Even when we extend the wavelength range to 5 to 14 μm, a high absorption rate of approximately 80% to 85% is still observed. Compared to high absorption but narrowband detector reported in the literature, this detector is promising to be used in spectrometer in detecting a variety of gases.[10] Here other than NH_3 and SF_6, it is suitable for more gas testing in this range, like N_O, NO_2, CH_4, O_3 etc.[11]

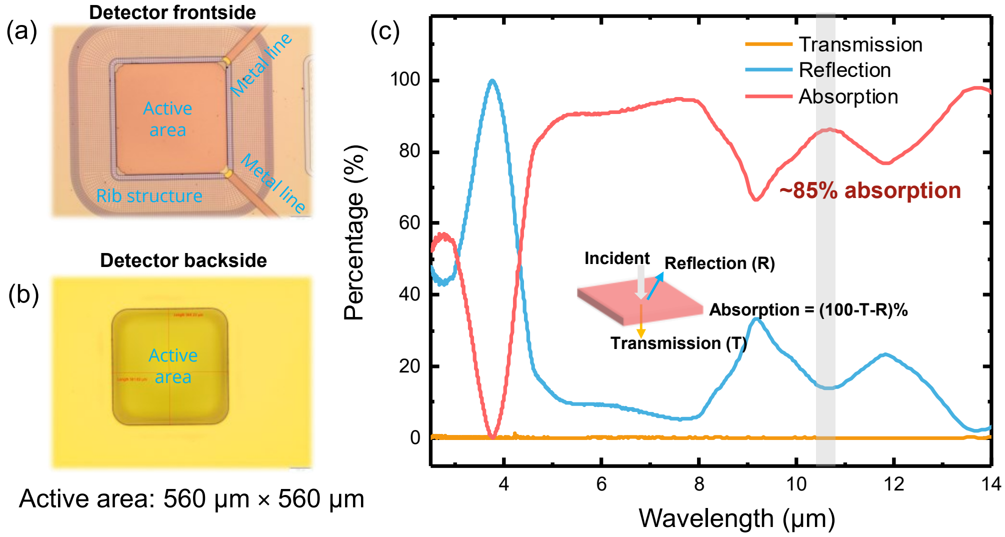

Figure 2. (a) Top and (b) bottom view microscope images of 20% ScAlN-based pyroelectric detector. (c) FTIR reflection, transmission and absorption spectra of the membrane pyroelectric detector in 2.5 μm to 14 μm wavelength range. Inset illustrates the detector slab and calculation equation.

3. SENSOR CHARACTERIZATIONS

3.1 Gas testing with 10 cm gas channel

As mentioned earlier, NH_3 gas testing presents significant challenges, primarily due to safety concerns associated with handling this hazardous gas. To address this, we initially focused on SF_6, which has a close absorption peak to NH_3 in the infrared spectrum, to validate the gas testing setup and establish a standardized system for NH_3 detection. Additionally, detecting SF_6 is of considerable importance, as it is a potential greenhouse gas to cause global warming. Figure 3a presents the sensor response to different concentrations of SF_6. The voltage drop relative to the N_2 baseline becomes more pronounced as the SF_6 concentration increases. This is because more light at the 10.7 μm wavelength is absorbed when the SF_6 concentration in the gas channel increases, leading to a weaker signal detected by the pyroelectric detector. In Figure 3b, the SF_6 concentration increases from 0 ppm to 200 ppm with a step size of 50 ppm. The plot is generated between the average value of the sensor voltages and the gas concentration within each time step. From the plot in Figure 3b, we can see the sensor voltage response decreases exponentially with the SF_6 concentration. The detection limit is calculated as 6 ppm according to [12]:

$$C_{limit} = 3\sigma/(\Delta V/\Delta C), \quad (2)$$

where σ is the voltage deviation at 0 ppm (pure N_2), and the $\Delta V/\Delta C$ is defined by the slope of fitted curve in Figure 3b, reflecting the sensitivity of the detector at low concentrations. The low detection limit indicates a good NDIR gas testing system for SF_6.

In Figure 3c and 3d, the NH_3 concentration varies over a range from 0 to 400 ppm in100 ppm step size. The voltage decreases linearly with the NH_3 concentration in Figure 3d. The difference in sensor voltage response to SF_6 and NH_3 concentrations is related to the gas absorption spectra and specific interactions between the gas and the sensor. The output voltage of SF_6 decreases exponentially, meaning that the response changes drastically with a certain change in gas concentration. This indicates that SF_6 has strong absorption. In contrast, NH_3, due to its weaker absorption, exhibits a linearly decreasing voltage response. Based on the fitted curves and the above equation in this section, the detection limit for NH_3 is calculated as 44 ppm. To further improve the detection limit of NH_3, we demonstrate sensor using 20 cm instead of 10 cm long gas channel.

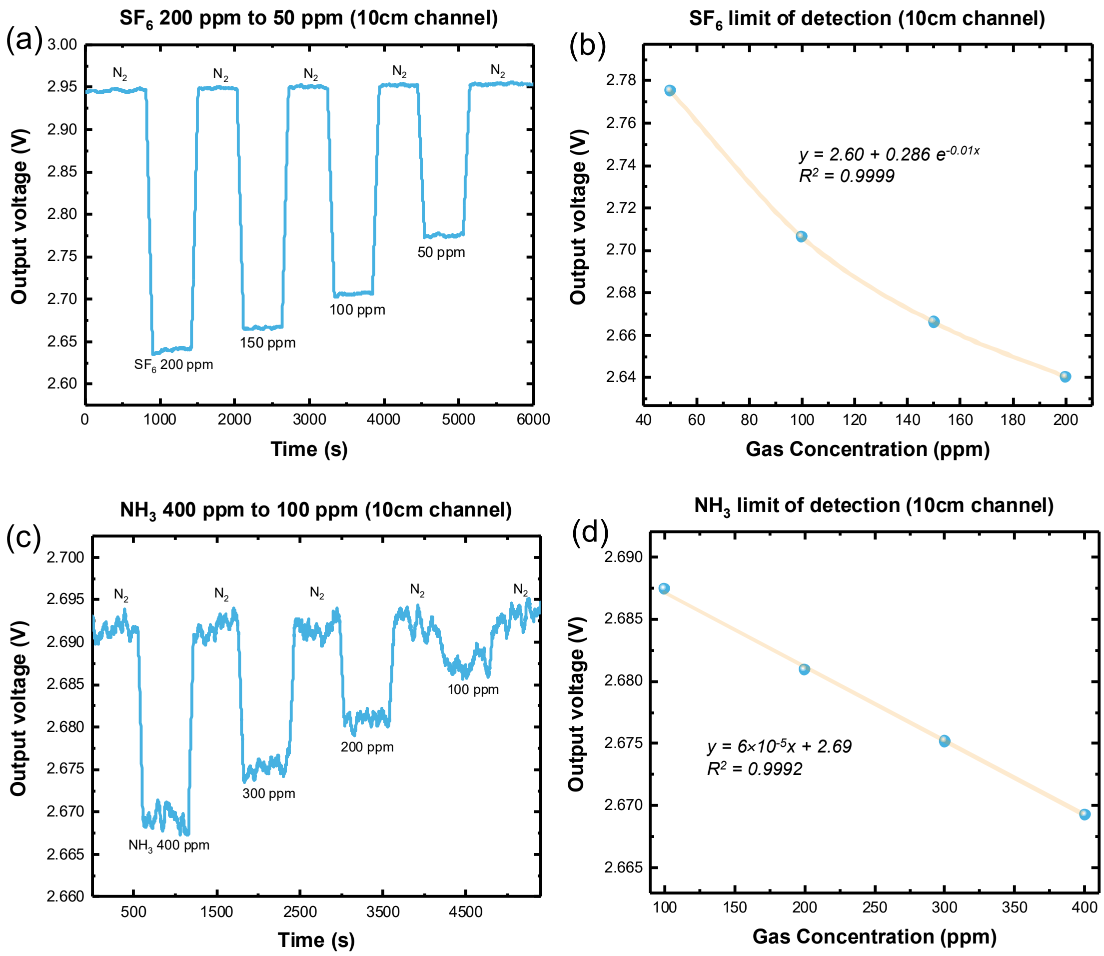

Figure 3. Gas testing characteristics on 10 cm testing setup. (a) Sensor voltage response to SF_6 from 0 (pure N_2) to 200 ppm in the time domain. (b) The output voltage to the SF_6 concentration changes over 50-200 ppm at steps of 50 ppm. (c) Sensor voltage response to NH_3 from 0 (pure N_2) to 400 ppm in the time domain. (d) The output voltage to the NH_3 concentration changes over 100-400 ppm at steps of 100 ppm.

3.2 Gas testing with 20 cm gas channel

Figure 4 shows the response of the gas sensor to different NH_3 concentrations in a 20 cm gas channel testing setup. Figure 4a presents the sensor's output signal cycled between different concentrations of NH_3 gas and N_2 gas. Figure 4b shows the sensor's response at different NH_3 concentrations. The experimental data agrees well with the modified Beer-Lambert law [9]:

$$gas\ response = span \times (1 - \exp(-\kappa\, l\, x)), \tag{3}$$

In the equation, x represents the NH_3 concentration, while κ is the effective absorption coefficient for NH_3. The optical gas channel, denoted as l, is approximately 0.2 m. The term *span* is a coefficient that reflects how much the infrared radiation is available to be absorbed by the gas. The experimental data are well fitted with determination coefficient - R^2 of 0.9791. With the fitted data, we calculated the *span* and κ as 0.014 and 0.025 respectively. This sensor exhibits a high effective absorption coefficient, higher than that observed in CO_2 studies,[9,13] while the intrinsic absorption of CO_2 is typically higher than that of NH_3. This indicates that the current sensor design enhances effective absorption through system design, thereby compensating for the intrinsic drawbacks.

Figure 4c shows the relationship between the sensor output voltage and NH_3 gas concentration, which helps in assessing the sensor's detection limit with 20 cm gas channel. Similar to 10 cm case in Figure 3d, an inverse linear relationship exists between the output voltage and gas concentration. The experimental data fit the linear equation well, with a coefficient of determination (R^2) of 0.99. According to the fitted curve, the detection limit decreased by more than 50%, from 44 ppm to 19 ppm, demonstrating a significant improvement in sensitivity.

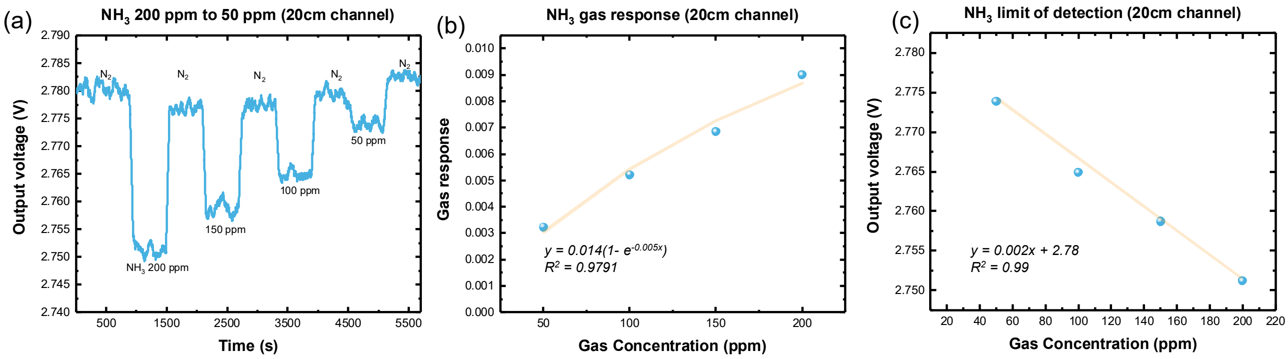

Figure 4. Gas testing characteristics on 20 cm testing setup. (a) Sensor voltage response to NH_3 from 0 (pure N_2) to 200 ppm in the time domain. (b) The gas response fitted to modified Beer- Lambert's law. (c) The output voltage to NH_3 over 50 to 200 ppm at a step of 50 ppm.

4. CONCLUSIONS

In this work, we develop an NDIR gas sensor capable of detecting low concentrations of gases, aiming to meet the growing demand for reliable leak sensors to monitor gaseous pollution and support hydrogen storage and transportation. This NDIR sensor, based on a 20% ScAlN pyroelectric detector, exhibits a high absorption of about 85% at the NH_3 and SF_6 characteristic absorption peaks. It shows high detection sensitivity, which can achieve detection limit of 19 ppm for NH_3 and 6 ppm for SF_6. The system demonstrates sufficient sensitivity to be deployed in various applications, offering an effective solution for real-time environmental monitoring and industrial safety control.

ACKNOWLEDGEMENTS

This research is supported by the National Research Foundation, Singapore, and A*STAR, Singapore under its Low-Carbon Energy Research (LCER) Phase 2 (Award no.: U2303D4001) for device fabrication and gas testing and Institute of Microelectronics, A*STAR (Agency for Science, Technology and Research) for fabrication and testing.

REFERENCES

[1] Zhao, Y., Liu, Y., Liu, Q., Zhao, J. and Zhang, Y., "Room-temperature operated fast reversible ammonia sensor based on hybrid optical fiber structure with temperature compensated function," Sensors and Actuators B: Chemical 408, 135472 (2024). doi: 10.1016/j.snb.2024.135472.

[2] Fang, X., Hu, X., Janssens-Maenhout, G., Wu, J., Han, J., Su, S., Zhang, J. and Hu, J., "Sulfur Hexafluoride (SF6) Emission Estimates for China: An Inventory for 1990–2010 and a Projection to 2020," Environ. Sci. Technol. 47(8), 3848–3855 (2013). doi: 10.1021/es304348x.
[3] Xing, Y., Urasinska-Wojcik, B. and Gardner, J. W., "Plasmonic enhanced CMOS non-dispersive infrared gas sensor for acetone and ammonia detection," 2018 IEEE International Instrumentation and Measurement Technology Conference (I2MTC), 1–5, IEEE, Houston, TX (2018). doi: 10.1109/I2MTC.2018.8409745.
[4] Dinh, T.-V., Choi, I.-Y., Park, B.-G., Lee, J.-H., Kim, I.-Y., Gil, H.-N., Lee, S.-W. and Kim, J.-C., "Development of a Negligible Zero-Drift NDIR Analyzer for Measuring NH3 Emitted from an Urban Household Solid Waste Incinerator," Atmosphere 12(7), 858 (2021). doi: 10.3390/atmos12070858.
[5] Dinh, T.-V., Choi, I.-Y., Son, Y.-S. and Kim, J.-C., "A review on non-dispersive infrared gas sensors: Improvement of sensor detection limit and interference correction," Sensors and Actuators B: Chemical 231, 529–538 (2016). doi: 10.1016/j.snb.2016.03.040.
[6] Zheng, S., Cai, H., Xu, L., Li, N., Gu, Z., Zhang, Y., Chen, W., Zhou, Y., Zhang, Q. and Lee, L. Y. T., "Silicon substrate-integrated hollow waveguide for miniaturized optical gas sensing," Photon. Res. 10(1), 261 (2022). doi: 10.1364/PRJ.439434.
[7] Manap, H., Dooly, G., O'Keeffe, S. and Lewis, E., "Ammonia detection in the UV region using an optical fiber sensor," 2009 IEEE Sensors, 140–145, IEEE, Christchurch, New Zealand (2009). doi: 10.1109/ICSENS.2009.5398215.
[8] Ng, D. K. T., Zhang, T., Siow, L. Y., Xu, L., Ho, C. P., Cai, H., Lee, L. Y. T., Zhang, Q. and Singh, N., "A functional CMOS compatible MEMS pyroelectric detector using 12%-doped scandium aluminum nitride," Applied Physics Letters 117(18), 183506 (2020). doi: 10.1063/5.0024192.
[9] Ng, D. K. T., Xu, L., Chen, W., Wang, H., Gu, Z., Chia, X. X., Fu, Y. H., Jaafar, N., Ho, C. P., Zhang, T., Zhang, Q. and Lee, L. Y. T., "Miniaturized CO2 Gas Sensor Using 20% ScAlN-Based Pyroelectric Detector," ACS Sens. 7(8), 2345–2357 (2022). doi: 10.1021/acssensors.2c00980.
[10] Zou, Y., Chen, S., Sun, J. and Zhou, S., "Mid-infrared pyroelectric detector with metasurface electrode for broadband enhanced absorption," J. Phys. D: Appl. Phys. 56(44), 445105 (2023). doi: 10.1088/1361-6463/aceb70.
[11] Popa, D. and Udrea, F., "Towards Integrated Mid-Infrared Gas Sensors," Sensors 19(9), 2076 (2019). , doi: 10.3390/s19092076.
[12] Tan, X., Zhang, H., Li, J., Wan, H., Guo, Q., Zhu, H., Liu, H. and Yi, F., "Non-dispersive infrared multi-gas sensing via nanoantenna integrated narrowband detectors," Nat Commun 11(1), 5245 (2020). doi: 10.1038/s41467-020-19085-1.
[13] Ng, D. K. T., Ho, C. P., Xu, L., Chen, W., Fu, Y. H., Zhang, T., Siow, L. Y., Jaafar, N., Ng, E. J., Gao, Y., Cai, H., Zhang, Q. and Lee, L. Y. T., "NDIR CO2 gas sensing using CMOS compatible MEMS ScAlN-based pyroelectric detector," Sensors and Actuators B: Chemical 346, 130437 (2021). doi: 10.1016/j.snb.2021.130437.